ÉCOLE POLYTECHNIQUE
FÉDÉRALE DE LAUSANNE

2004.7

LESO-PB

Dielectric Interference Layers for Solar Thermal Collectors

Schueler A., Roecker C., Scartezzini J.-L. (EPFL)
Boudaden J., Oelhafen P. (Universität Basel)

Proceedings of EUROSUN 2004, Freiburg in Brisgau (D)

June 2004

DIELECTRIC INTERFERENCE LAYERS FOR SOLAR THERMAL COLLECTORS

J. Boudaden[1] and P. Oelhafen[1],

[1] Institut für Physik, University of Basel, Klingelbergstrasse 82, CH-4056 Basel, Switzerland
Tel: 41-61-267-37-15, Fax: 41-61-267-37-82, jamila.boudaden@unibas.ch

A. Schüler[2], C. Roecker[2] and J. - L. Scartezzini[2]

[2] Laboratoire d'Energie Solaire et de Physique du Bâtiment LESO-PB, Ecole Polytechnique Fédérale de Lausanne (EPFL), Bâtiment LE, CH-1015 Lausanne, Switzerland

Abstract

Our aim is to study the possibility of integrating dielectric multilayer films deposited on glass substrates as a colored glazed cover for thermal solar collectors and building faces. The cover glass should ideally reflect only a narrow band of visible light while transmitting the rest of the sunlight spectrum to minimize energy loss. A compromise between the visible reflectance and the solar transmission has to be found. In our multilayer interference filters, we used two materials having respectively a high and a low refractive index. We studied two cases: Al_2O_3/SiO_2 and TiO_2/SiO_2. The thin films were deposited by reactive magnetron sputtering. In-situ XPS characterizations were carried out for each film by transferring the sample from the deposition chamber to an ultra-high vacuum analysis chamber without breaking the vacuum. The growth rate of TiO_2, SiO_2 and Al_2O_3 single layers on Si substrates were monitored by in-situ laser reflectometry. Spectroscopic ellipsometry was used to determine the optical constants and the thicknesses of every individual dielectric layer. Reflectivity measurements of the experimentally realized dielectric multilayers deposited on glass substrates confirmed their transparency and their good accordance with the simulation. The multilayers were also characterized by their solar transmission, visible reflectance and a factor of merit.

Keywords: multilayer, dielectric oxides, thermal solar collectors

1. INTRODUCTION

Transparent oxide films are widely employed as antireflection or high reflection coatings [1,2], band-pass filters [3] and narrow-band-filters [4] in various optical and electronic devices. The performances of these devices are based on interference effects obtained by alternating layers of high and low refractive indices.
Nowadays different deposition methods exist to produce dielectric oxide films. Thin film evaporation underwent rapid development and became a standard method for optical coatings [5]. Afterwards, alternative methods such as chemical vapor deposition [6], dip coating [7], sol gel method [8] and reactive sputtering [9] have been extensively studied.

The latter allows large area coatings and thicknesses uniformity combined with high growth rate deposition [10].
In our case, reflecting multilayers are used as a cover for solar collectors. A large fraction of power from the solar radiation must be transmitted through the coatings. The transparency of the film permits avoiding absorption energy losses within the coating. At the same time, the multilayer films should present a narrow reflection band in the visible range. This selective reflection fixes the color of the reflected light. A combination of different refractive indexes and thicknesses makes it possible to realize a wide range of reflected colors with an acceptable solar transmission [11].
In this work, we report an experimental study for the preparation of optical coatings based on TiO_2/SiO_2 and Al_2O_3/SiO_2 multilayer dielectric films realized by reactive magnetron sputtering by depositing alternating layers of two materials. During the experimental realization, some important requirements must be fulfilled. The deposition technique must allow good control and reproducibility of the optical properties of any individual thin film combined with a high deposition rate. The interface between two layers should be as smooth as possible. To meet the above conditions TiO_2, SiO_2 and Al_2O_3 are considered a suitable materials to cover solar thermal collectors.

2. EXPERIMENT

2.1 Thin film deposition and photoelectron spectroscopy

06

The titanium oxide, silicon oxide and aluminium oxide thin films were prepared by reactive magnetron sputtering in a high vacuum deposition chamber using an Ar/O_2 gas mixture. The mass flow ratio is set to 35:5 for titanium and silicon oxide and to 37:3 for aluminium oxide. The magnetrons are driven by bipolar-pulsed power for the Ti target (50 kHz at 200 W) and for the Al target (50 kHz at 150 W) and by medium frequency RF power (13.5 kHz at 100 W) for Si target. During the thin film deposition carried out at room temperature, the grounded substrates face the target at a distance between 5 and 8 centimeters. A working pressure of around 3×10^{-3} mbar is adjusted by throttling the pumping system. TiO_2, SiO_2 and Al_2O_3 films are deposited on glass AF45 and monocrystalline silicon (with its native oxide) substrates 4 x 4 cm^2 for the characterization optical techniques. For the in-situ photoelectron spectroscopy thin films are deposited on sputter cleaned copper substrates.
The high vacuum deposition chamber is connected to an ultrahigh vacuum (UHV) electron spectrometer. Samples can be transferred from one system to the other without breaking the vacuum to get chemical information about the deposited films. The electron spectrometer is equipped with a hemispherical analyzer (Leybold EA 10/100) and a X-ray source for core level spectroscopy (X-ray photoelectron spectroscopy XPS: Mg $K\alpha$ excitation, $h\upsilon$ = 1253.6 eV). The typical resolution is 0.8 eV for the XPS measurements. A gold sample with the Au $4f_{7/2}$ core level signal at 83.9 eV binding energy is used as a reference for the electron energy calibration.
Ti 2p, Si 2p, Al 2p and O1s core levels were recorded in the case of TiO_2, SiO_2 and Al_2O_3 to determine the chemical composition for each layer. Atomic concentration ratios were calculated by integrating the peaks area after subtracting a Shirley background [12]. From the photoionization cross-sections given by [13], the atomic concentration at the films surface is calculated using UNIFIT program [14]. In our deposition conditions, the stoichiometry of the TiO_2, SiO_2 and Al_2O_3 films is reproducible.

2.2 Optical characterization

The optical reflectivity of a laser beam is measured continuously during the film deposition in order to determine the deposition rate and the optical constants *n* and *k* at one wavelength. The analysis of the data is performed using the reflectivity formula of a single layer on the substrate for the numerical fitting [15]. The experimental set up involves an incident laser beam at 532 nm and the detection of the reflected intensity with a synchronous modulator [16].
Spectroscopic ellipsometry is a non-destructive optical measurement of the polarization change occurring when the incident light interacts with layers. The two ellipsometric functions Δ and Ψ are measured at each wavelength across the spectral range of interest of the reflected light. The optical constants *n* and *k* and the thicknesses of any individual thin films inside a multilayer coating are determined from a model-based regression limited to the experimental available data. For this reason, ellipsometry is performed at different angle of incidence. The films on silicon substrates with its native oxide are subjected to ellipsometry measurements, performed by ellipsometer (SENTECH SE 850) in the range of 300 - 850 nm with variable angle of incidence ranging between 40° and 70° by steps of 10°.
The total hemispherical reflectivity at 7° angle of incidence and transmission at 0° angle of incidence measurements in the UV, VIS and NIR are performed on a Varian Cary 5 spectrophotometer.
Silicon wafers have been used as a substrate for in-situ real-time laser reflectometry and ex-situ ellipsometry while glass substrates have been used for ex-situ spectrophotometry.

3. RESULTS AND DISCUSSION

3.1 Laser Reflectometry

The reflectivity data at 532 nm were monitored as a function of time during the deposition of TiO_2, SiO_2 and Al_2O_3 films on silicon substrates using the laser light polarization parallel to the incidence plane.
The obtained curves can be interpreted in a qualitative way. The experimental curves show oscillations with constant amplitude, indicating the transparency of the film. Hence, the extinction coefficient *k* at 532 nm is zero as expected. A quantitative determination of the optical constants is done by numerical fitting of the experimental data using the reflectivity formula of a one layer on substrate model. In a straightforward way, in-situ laser reflectometry fits provide the growth rate v_d, the refractive and extinction indexes at one wavelength (532 nm) as summarized in table 1.

	n	v_d [nm/min]
TiO_2	2.2	1.2
SiO_2	1.47	7.6
Al_2O_3	1.5	25

Table 1. Optical constants and deposition rate of TiO_2, SiO_2 and Al_2O_3 thin films using laser reflectometry.

3.2 Ellipsometry of individual layers

The ellipsometric data consist of the ψ and Δ spectra in the range 300 to 850 nm for different incident angles between 40° and 70°. Consequently, we have made a systematic study of the optical properties of individual dielectric layer for TiO_2, SiO_2 and Al_2O_3. The model consists of a single uniform film on silicon substrate. These data were fitted with a widely used Cauchy dispersion formula for TiO_2, SiO_2 and Al_2O_3, where the refractive index n and extinction coefficients k are given by:

$$n(\lambda) = n_0 + C_0 \frac{n_1}{\lambda^2} + C_1 \frac{n_2}{\lambda^4} \quad (1)$$

$$k(\lambda) = k_0 + C_0 \frac{k_1}{\lambda^2} + C_1 \frac{k_2}{\lambda^4} \quad (2)$$

n_i, k_i, C_i are constants and λ is the wavelength in nm. We take $C_0 = 10^2$ and $C_1 = 10^7$, which are mostly used, to avoid large values of n_1, k_1, n_2 and k_2.

The films were modeled as homogeneous dielectric layers on a semi-infinite silicon substrate. A native silicon dioxide interlayer was included in the model. Surface roughness was neglected.

The experimental ψ and Δ for deposited TiO_2, SiO_2 and Al_2O_3 on silicon substrate combined with the best theoretical fits using the Cauchy dispersion model, permits to determine the optical properties of individual films. A good agreement between the fit and the experimental data is observed between 250 and 850 nm for SiO_2 and Al_2O_3, and above 350 nm in the case of TiO_2 thin film, which confirms our results previously obtained for the same deposition conditions [11].

Figure 1 shows the refractive index n as a function of the wavelength in the UV-Vis for TiO_2, SiO_2 and Al_2O_3 on silicon substrate. The results of the fit parameters confirm that no absorption occurs in the films. It should be noted here that the thicknesses of dielectric layers are in a good agreement and are within 5% of the determined one by the laser reflectometry.

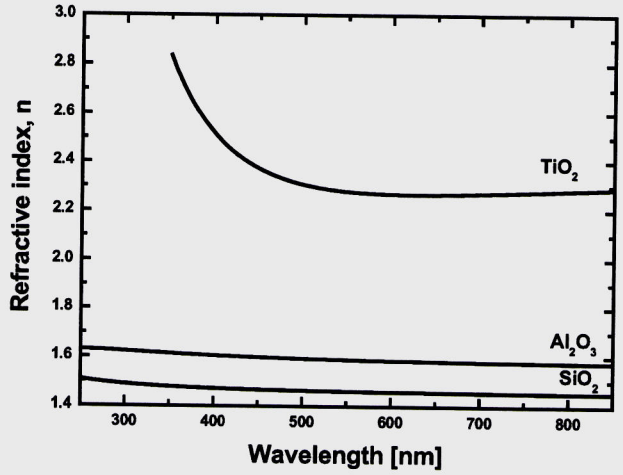

Figure 1. Refractive index of individual layers TiO_2, Al_2O_3 and SiO_2 in the visible range deduced from ellipsometry data.

3.3 Total hemispherical reflectivity

The total hemispherical reflectivity $R(\lambda)$ and transmission $T(\lambda)$ for single-layer on glass samples show a quasi-zero absorption of the films, confirming the previous results from laser reflectometry and spectroscopic ellipsometry methods. The theoretical curves of Figs. 2 and 3 are calculated using the experimental optical constants determined by spectroscopic ellipsometry on single-layer samples. In our model, we suppose homogenous layers and sharp interfaces.

Figure 2 represents the total hemispherical reflectivity of TiO_2/SiO_2 multilayers formed by three and five alternating layers of TiO_2/SiO_2. The thicknesses of the layers are indicated in table 2. We observe a reflectivity peak in the visible range. The peak position determines the color of the multilayer film. The dotted lines indicate the theoretical reflectivity. We observe a good agreement between the experimental and the theoretical values. The reflectivity peak position, its maximum value and its FWHM depend on the layer thicknesses and on the number of layers. In general, at one wavelength the reflectivity peak maximum increases with increasing layer number.

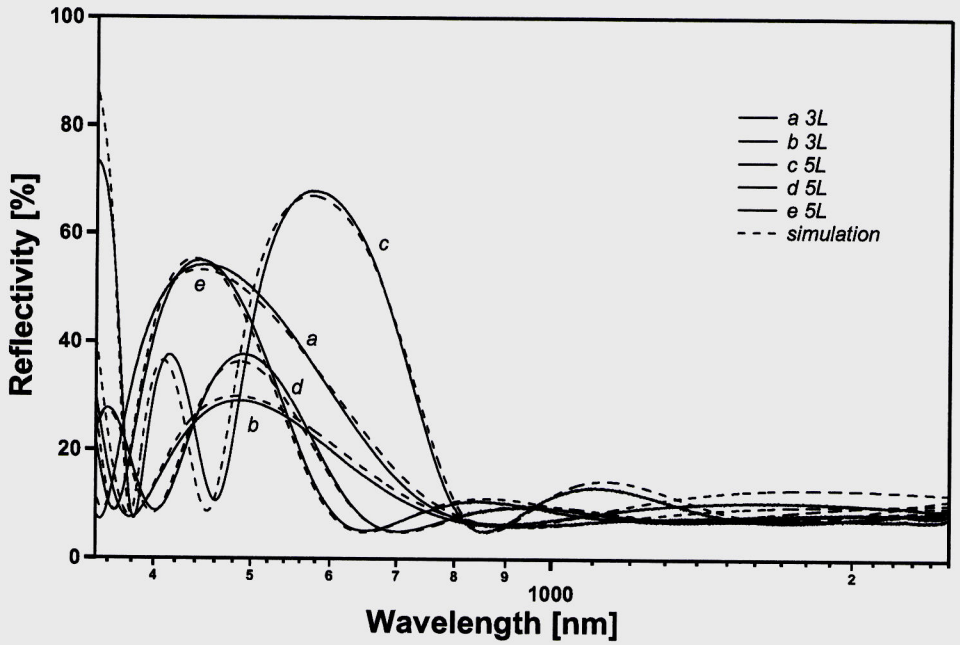

Figure 2. Measured total reflectivity of TiO_2/SiO_2 multilayers (solid lines) combined with the theoretical one (dotted lines)

Figure 3 shows the total hemispherical reflectivity of Al_2O_3/SiO_2 multilayers formed by an increasing number of alternating layers having the same thicknesses. The dotted lines indicate the theoretical reflectivity increasing with the layer number. This evolution shows the same tendency as previously presented results obtained by using the simplified model of constant refractive indexes [17].

The thicknesses of the individual layers of Fig. 3 are indicated in table 3. The peak position is relatively constant and its maximum value increases by increasing the number of alternating layers. The disagreement between the experimental and calculated values for

the nine-layers samples can be explained by the long deposition time and an eventual change of the deposition conditions.

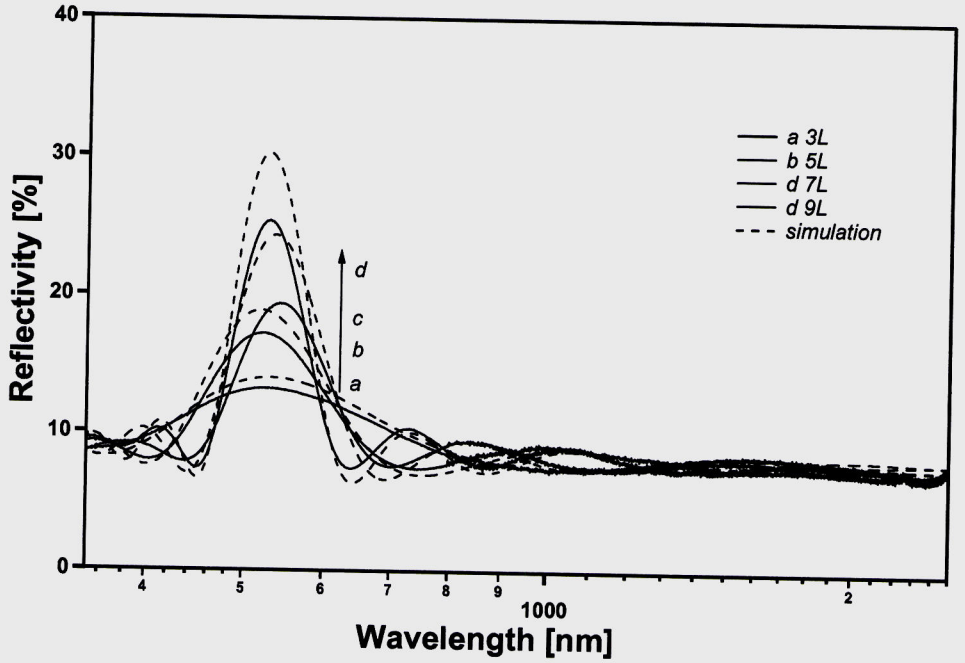

Figure 3. Measured total reflectivity of Al_2O_3/SiO_2 multilayers (solid lines) combined with the theoretical one (dotted lines)

3.4 Global performances

In order to take account of the solar spectrum, a multilayer sample is characterized by its solar transmission T_{sol}, its solar reflectivity R_{sol} defined respectively by the following relations:

$$T_{sol} = \frac{\int T(\lambda) I_{sol}(\lambda)\, d\lambda}{\int I_{sol}(\lambda)\, d\lambda} \qquad (3)$$

$$R_{sol} = \frac{\int R(\lambda) \cdot I_{sol}(\lambda) d\lambda}{\int I_{sol}(\lambda) d\lambda} \qquad (4)$$

We note here I_{sol} the intensity of the solar spectrum AM1.5. The integration range is given by the limits of the solar spectrum. The visible reflectance R_{vis} is determined from the photopic luminous efficiency function $V(l)$, the standard illumination $D_{65}(\lambda)$ and the hemispherical reflectivity $R(\lambda)$:

$$R_{vis} = \frac{\int R(\lambda) \cdot D_{65}(\lambda) \cdot V(\lambda) d\lambda}{\int D_{65}(\lambda) \cdot V(\lambda) d\lambda} \quad (5)$$

For the theoretical case of a delta-distribution-shaped reflectivity, Schüler et al. [18] introduced a merit factor *M* defined as the ratio of the visible reflectance R_{vis} and the solar reflectivity R_{sol}. *M* is then large for a high visible reflectance or low solar energy losses and consequently describes the energy efficiency of the visual perception.
Numerical simulations allow optimizing the reflectivity and transmission of the multilayer films as a function of the film thicknesses, the refractive indexes and the number of alternating layer. They show a correlation between the difference of the refractive index of the two materials. For example, a lower refractive index difference increases the optimal thicknesses of the individual layers and the layer number, but the solar transmission is high. The simulation optimization results based on the experimental optical constants of single layers will be published elsewhere [19].
Table 2 shows the solar transmission, the solar reflectivity, the relative visible reflectance and the merit factor $M = R_{vis}/R_{sol}$ in the case of the TiO_2/SiO_2 multilayers. We indicated the experimental and calculated values. We see that for a given number of alternating layers, it is always possible to obtain either a high solar transmission or a high relative visible reflectance by adapting the thicknesses of both oxide materials. In order to obtain the best compromise between the energy losses by reflectivity and the visual effect, both parameters have to been optimized. Samples *a* and *c* show that the merit factor is not a sufficient indicator and one has to take into account the absolute R_{sol}. In fact, in these examples, the solar transmission is low and results in a uselessly high visible reflectance.

		d_{TiO2} [nm]	d_{SiO2} [nm]	T_{sol} exp	T_{sol} theo	R_{sol} exp	R_{sol} theo	R_{vis} exp	R_{vis} theo	R_{vis}/R_{sol} exp	R_{vis}/R_{sol} theo
2L		27	195	88.1	87.6	12	12.4	19.8	20.1	1.65	1.62
3L	*a*	30	122	77.8	77.2	22.1	22.8	39.4	39.1	1.78	1.71
		63	73	66	67.3	33.7	32.7	64.1	58.7	1.90	1.80
	b	18	160	85.8	84.7	14.3	15.3	24.2	25.2	1.70	1.65
5L	*c*	35	148	70.7	69.9	29.2	30.1	60.5	61.1	2.10	2.00
	d	14	155	85.5	85.9	14.2	14.1	23.3	24.8	1.83	1.75
	e	19	130	82.9	82.9	16.9	17.1	23.3	22.2	1.37	1.30

Table 2. Measured parameters (thicknesses, solar transmission and reflectivity, visible reflectance and merit factor) of TiO_2/SiO_2 multilayers combined with the same theoretical parameters

Table 3 shows the solar transmission, the solar reflectivity, the relative visible reflectance and the merit factor M in the case of the Al_2O_3/SiO_2 multilayers. The solar transmission is slightly decreasing by increasing layer number, but stays at a high level superior to 89%, which is comparable to the solar transmission of uncoated glass (92 %). As mentioned above, this is due to the small refractive index difference between SiO_2 and Al_2O_3. The relative visible reflectance and hence the factor M increases.
The result shows that the prepared coatings can meet the requirements for obtaining different reflected colors. More efforts are needed to improve at the same time the solar transmission and the visible reflectance by considering other oxides and by optimizing the layer thicknesses.

		d_{Al2O3} [nm]	d_{SiO2} [nm]	T_{sol} exp	T_{sol} theo	R_{sol} exp	R_{sol} theo	R_{vis} exp	R_{vis} theo	R_{vis}/R_{sol} exp	R_{vis}/R_{sol} theo
3L	*a*	83	95	90.5	90	9.8	10	12.7	13.5	1.3	1.34
5L	*b*	83	92	89.9	89.6	10.2	10.4	15.2	16.4	1.5	1.58
7L	*c*	80	91	89.7	89.1	10.3	10.9	16.7	20	1.63	1.84
9L	*d*	80	90	89.4	88.8	10.7	11.2	18.7	21.7	1.74	1.93

Table 3. Measured parameters (thicknesses, solar transmission and reflectivity, visible reflectance and merit factor) of Al_2O_3/SiO_2 multilayers combined with the same theoretical parameters

4. CONCLUSION

In this work, colored glass to cover solar collectors has been obtained by alternative deposition of dielectric layers with high and low refractive indices. The stoichiometry was first checked by XPS. The deposition rate has been controlled by in-situ laser reflectometry and confirmed by ex-situ ellipsometry for complex systems with several layers. The optical properties of individual oxides of titanium, silicon and aluminium have been determined. A Cauchy dispersion model is adequate for extracting the refractive and extinction index in the case of reactive magnetron sputtering deposition.

The reflectivity and the solar transmission depend on the thicknesses and the number of the alternative dielectric layers. The fabricated multilayers fulfilled the fixed requirements: quasi-zero absorption, reflectivity peak in the visible, solar transmission above 85% up to 89% and an acceptable visible reflectance.

More effort will be directed to study the lifetime of the multilayer coatings by aging tests in order to investigate their applicability for architectural integration in buildings.

ACKNOWLEDGEMENTS

The authors wish to thank Dr. M. Ley for helpful discussions and R. Steiner for the technical support. This work is supported by the Swiss Federal Office of Energy and the Swiss National Science Foundation.

REFERENCES

[1] D. Bhattacharyya, N.K. Sahoo, S. Thakur, N.C. Das, Vacuum 60 (2001) 419-424.

[2] H. Selhofer and R. Müller, Thin Solid Films 351 (1999) 180-83.

[3] C. Garapon, J. Mugnier, G. Panczer, B. Jacquier, C. Champeaux, P. Marchet and A. Catherinot, Appl. Surf. Science 96-98 (1996) 836-841.

[4] M.F. Ouellette, R.V. Lang, K.L. Yan, R.W. Bertram, R.S. Owies and D. Vincent, J. Vac. Sci. Technol. A. 9 (1991) 1188-92.

[5] Z.D.X. Guangzhong and L. Wi, Vacuum 42 (1991) 1087.

[6] C. Martinet, V. Paillard, A. Gagnaire and J. Joseph, J. Non-Cryst. Solids 216 (1997) 77-82.

[7] H. Köstlin, G. Frank, H. Auding and G. Hebbinghaus, J. Non-Cryst. Solids 218 (1997) 347-53.

[8] W. Que, W. Sun, Y. Zhou, Y.L. Lam, Y.C. Chan and C.H. Kam, Thin Solid Films 359 (2000) 177-83.

[9] R.J. Hill, J. Non-Cryst. Solids 218 (1997) 54-57.

[10] M. Vergöhl, N. Malkomes, T. Staedler, T. Matthée and U. Richter, Thin Solid Films 351 (1999) 42-47.

[11] J. Boudaden, R. S.-C. Ho, P. Oelhafen, A. Schüler, C. Roecker and J.-L. Scartezzini, to be published in Solar Energy Mater. Solar Cells (2004).

[12] D.A. Shirley, Phys. Rev. B. 5 (1972) 4709-14.

[13] J.J. Yeh and I. Lindau, Atomic Data and Nuclear Data Tables 32 (1985) 1-3.

[14] R. Hesse, T. Chassé, R. Szargan , Unifit 2002 - universal analysis software for photoelectron spectra, Anal. Bioanal. Chem. 375 (2003) 85-63.

[15] O.S. Heavens, Optical properties of thin solid films, (New York, 1991).

[16] A. Schüler, C. Ellenberger, P. Oelhafen, C. Haug and R. Brenn, J. Appl. Phys. 87 (2000) 4285-92.

[17] A. Schüler, C. Roecker, J. Boudaden, P. Oelhafen, J. - L. Scartezzini, Proceedings of the CISBAT conference, 8 Oct. (2003) Lausanne, Switzerland.

[18] A. Schüler, C. Roecker, J.-L. Scartezzini, J. Boudaden, I. R. Videnovic, R. S.-C. Ho, P. Oelhafen, to be published in Solar Energy Mater. Solar Cells (2004).

[19] J. Boudaden et al., to be submitted.